H(+)/Cl(-) exchange transporter 7 promotes lysosomal acidification-mediated autophagy in mouse cardiomyocytes

JIEZHI LIN[1,2*], JINYU WEI[1,3*], YANLING LV[1], XINGYUE ZHANG[1], RUO FAN YI[1], CHEN DAI[4], QIONG ZHANG[1], JIEZHI JIA[1], DONGXIA ZHANG[1] and YUESHENG HUANG[1,5]

[1]Institute of Burn Research, State Key Laboratory of Trauma, Burns and Combined Injury, Southwest Hospital, Third Military Medical University, Chongqing 400038; [2]Military Burn Center, The 963rd (224th) Hospital of People's Liberation Army, 963rd Hospital of Joint Logistics Support Force of PLA, Jiamusi, Heilongjiang 154007; [3]Dermatology Department, The 920th Hospital of People's Liberation Army, 920th Hospital of Joint Logistics Support Force of PLA, Kunming, Yunnan 650100; [4]Orthopedics and Trauma Department, The 963rd (224th) Hospital of People's Liberation Army, 963rd Hospital of Joint Logistics Support Force of PLA, Jiamusi, Heilongjiang 154007; [5]Department of Wound Repair, Institute of Wound Repair, Shenzhen People's Hospital, The First Affiliated Hospital of Southern University of Science and Technology, and The Second Clinical Medical College of Jinan University, Shenzhen, Guangdong 518020, P.R. China

Received April 4, 2020; Accepted November 6, 2020

DOI: 10.3892/mmr.2021.11861

Abstract. Autophagy protects cardiomyocytes in various pathological and physiological conditions; however, the molecular mechanisms underlying its influence and the promotion of autophagic clearance are not completely understood. The present study aimed to explore the role of H(+)/Cl(-) exchange transporter 7 (CLC-7) in cardiomyocyte autophagy. In this study, rapamycin was used to induce autophagy in mouse cardiomyocytes, and the changes in CLC-7 were investigated. The expression levels of CLC-7 and autophagy-related proteins, such as microtubule associated protein 1 light chain 3, autophagy related 5 and Beclin 1, were detected using western blotting or immunofluorescence. Autolysosomes were observed and analyzed using transmission electron microscopy and immunofluorescence following CLC-7 silencing with small interfering RNAs. Cellular viability was assessed using Cell Counting Kit-8 and lactate dehydrogenase assays. Lysosomal acidification was measured using an acidification indicator. Increased CLC-7 co-localization with lysosomes was identified during autophagy. CLC-7 knockdown weakened the acidification of lysosomes, which are the terminal compartments of autophagy flux, and consequently impaired autophagy flux, ultimately resulting in cell injury. Collectively, the present study demonstrated that in cardiomyocytes, CLC-7 may contribute to autophagy via regulation of lysosomal acidification. These findings provide novel insights into the role of CLC-7 in autophagy and cytoprotection.

Correspondence to: Professor Dongxia Zhang or Professor Yuesheng Huang, Institute of Burn Research, State Key Laboratory of Trauma, Burns and Combined Injury, Southwest Hospital, Third Military Medical University, 30 Gaotanyan Road Shapingba, Chongqing 400038, P.R. China
E-mail: dxzhangswh@163.com
E-mail: yshuangtmmu@163.com

*Contributed equally

Abbreviations: CLC-7, H(+)/Cl(-) exchange transporter 7; v-ATPase, vacuolar-type H+-ATPase; LC3, microtubule associated protein 1 light chain 3; p62, sequestosome 1; LAMP1, lysosomal-associated membrane protein 1; CQ, chloroquine

Key words: CLC-7, rapamycin, lysosomal acidification, autophagy, cardiomyocyte

Introduction

Autophagy maintains cellular homeostasis via the recycling of long-lived proteins and removal of damaged organelles (1-3), such that it protects cardiomyocytes from damage and death, as well as improves cardiac function in several pathological conditions, including traumatic shock, ischemia-reperfusion and coronary artery disease, amongst others (4-9). However, previous studies have reported that activated myocardial autophagy results in cardiomyocyte death in rats following severe burns, instead of protecting cardiac function (6,10). Although autophagy is active, redundant autophagosome accumulation is found in various types of pathological conditions, such as oxidative stress and acute hypoxia, leading to subsequent autophagic cell death (11-14). Eliminating autophagosome accumulation and enhancing the activity of autophagy-related pathways significantly improves cardiomyocyte viability (15). Thus, improvement of autophagy flux is important for protecting cells from damage when under stress.

Lysosomes, which contain hydrolases that degrade endocellular macromolecules, are essential in the autophagy pathway (16). Impaired lysosomal function leads to

autophagosome accumulation and subsequent cardiomyocyte death, which has been observed in various pathological conditions including hypoxia, ischemia-reperfusion and fibrosis (14,17,18). Therefore, studying the mechanism of lysosomal acidification may identify potential avenues for treatment of diseases that result from excess cardiomyocyte death. In lysosomes, the activation of hydrolases requires a low luminal pH (19). Transporters, such as vacuolar-type H^+-ATPase (v-ATPase) and Cl^-, K^+ and Na^+ channels, participate in maintaining the luminal pH (19,20).

H(+)/Cl(-) exchange transporter 7 (CLC-7) is a $2Cl^-/1H^+$ antiporter that is primarily found in late endosomes and lysosomes (21,22). CLC-7 regulates Cl^- conductance, which enables osteoclast ruffled border ATPases to facilitate efficient proton pumping (23). The ruffled border delivers HCl and proteases to resorption lacuna between osteoclasts and the bone (23,24). The low luminal pH caused by HCl serves a fundamental role in dissolving and absorbing bone material (23). Loss of CLC-7 transporters leads to lysosomal storage diseases and osteopetrosis (18,23-25). However, the mechanism of CLC-7 in lysosomes is contested. CLC-7 knockdown was shown to inhibit lysosomal acidification in HeLa cells and primary mouse microglia, as well as isolated lysosomes (19,21,26). However, lysosomal pH changes in CLC-7 knockout mice were not significant (18,23-25,27). Furthermore, to the best of our knowledge, there are no studies on the role of CLC-7 in autophagy. Rapamycin, a well-known activator of autophagy, results in activation of autophagy by specifically inhibiting mTOR function (1,28). In the present study, a model of autophagy using rapamycin-treated neonatal mouse cardiomyocytes was established, and the potential roles of CLC-7 in lysosomal acidification and autophagy were investigated.

Materials and methods

Chemicals and reagents. Antibodies against CLC-7 (cat. no. GTX55139; GeneTex, Inc.), sequestosome 1 (p62; cat. no. 23214; Cell Signaling Technology, Inc.), α-tubulin (cat. no. 11224-1-AP; ProteinTech Group, Inc.), autophagy related 5 (ATG5; cat. no. 10181-2-AP; ProteinTech Group, Inc.), microtubule associated protein 1 light chain 3 (LC3; cat. no. PA1-46286; Thermo Fisher Scientific, Inc.), lysosomal-associated membrane protein 1 (LAMP1; cat. no. ab25245; Abcam), mTOR (cat. no. 2983; Cell Signaling Technology, Inc.), phospho (p)-mTOR (Ser2448; cat. no. 5536; Cell Signaling Technology, Inc.), Beclin-1 (cat. no. ab207612; Abcam) and cathepsin D (cat. no. ab75852; Abcam) were utilized. In addition, horseradish peroxidase (HRP)-conjugated anti-rabbit secondary antibody (cat. no. SA00001-2; ProteinTech Group, Inc.), rapamycin (cat. no. S1039; Selleck Chemicals) and chloroquine (CQ; cat. no. S8808; Selleck Chemicals) were used in this study. Cell culture reagents were purchased from Thermo Fisher Scientific, Inc. RNAlater™ Solution (cat. no. AM7020; Thermo Fisher Scientific, Inc.), TRIzol® reagent (cat. no. 15596018; Invitrogen; Thermo Fisher Scientific, Inc.), QuantiNova™ reverse transcription kit (cat. no. 205411; Qiagen, Inc.) and QuantiNova™ SYBR® Green PCR kit (cat. no. 208054; Qiagen, Inc.) were used for reverse transcription-quantitative (RT-q)PCR. All other reagents were provided by Sigma-Aldrich (Merck KGaA), unless otherwise stated.

Primary cell culture. Ventricular muscles of neonatal C57BL/6J mice (age, 1 day old; male and female; weight, 1.5-1.8 g) from the Experimental Animal Center of the Army Medical University, were digested with trypsin and cultured following the protocols published previously (29). Mice were given food and water freely and were kept in an environmental of temperature (20-22˚C), humidity (50-60%) and a 12/12 h light/dark cycle. According to the grouping, cellular survival status and experimental repetitions, 126 neonatal mice were sacrificed in this research. There were no other causes of mortality of mice other than execution for the experiment (extracting myocardium). Before execution, their skin condition (redness of the skin) and autonomous movements were monitored, and a warm environment was required. Euthanasia of mice was performed by decapitation following anesthesia. Mice were anesthetized by intraperitoneal injection of pentobarbital sodium (50 mg/kg). When no spontaneous or stimulus-induced movement and squeaks were detected, cerebral palsy was considered to be effective, and the mice were decapitated. After soaking with 75% ethanol, the chest was opened and the heart was extracted instantly. It took ~3 min from drug injection to observing completely successful anesthesia, and then to extracting the heart.

Cardiomyocytes were cultured in DMEM-F12 (Hyclone; Cytiva), supplemented with 5-bromode-oxyuridine (Brdu; 31 mg/l; Sigma-Aldrich; Merck KGaA), 10% (v/v) heat-inactivated FBS (Gibco; Thermo Fisher Scientific, Inc.), penicillin G (100 U/ml) and streptomycin (100 mg/ml; Sigma-Aldrich; Merck KGaA), and maintained at 37˚C in a 5% CO_2 incubator. 5Brdu supplement can effectively inhibit the growth of myocardial fibroblasts, but has no obvious effect on cardiomyocytes vitality, and has been widely used in the study of primary myocardial cell culture (29-31). Treatment with reagents [rapamycin, CQ and small interfering (si)RNA] for experimental analysis was performed after 3 days of culture. The reagents treatment processes were mentioned in following experimental methods.

Establishment of the autophagy model. On the 3rd day of cell culture, cardiomyocyte beating was viewed under an optical microscope (magnification, x400). Fast and rhythmic cellular beats were indicative of a healthy state (32). The medium was replaced with rapamycin-containing (200 nM) or DMSO-containing (same amount as the former) medium and cultured for different time periods (37˚C for 1, 3 and 6 h). Expression levels of autophagy-related proteins were detected using western blotting to determine successful establishment.

Autophagy blockage. CQ was used to block autophagy. The medium was replaced with CQ-containing (100 nM) medium and cardiomyocytes were pretreated for 2 h at 37˚C prior to activation of autophagy with rapamycin treatment. The blocking effect of CQ on cardiomyocytes autophagy was detected using western blotting and lysosomal acidification assay.

CLC-7 knockdown. The CLC-7-specific siRNAs were designed, synthesized and verified by Shanghai GenePharma Co., Ltd.

Non-targeting controls (negative control siRNA) were used. The sequences used were: CLC-7 siRNA1 (S1) sense, 5'-GCU CCUCUCCCUCAAGUAUTT-3' and antisense, 5'-AUACUU GAGGGAGAGGAGCTT-3'; CLC-7 siRNA2 (S2) sense, 5'-GCAUCUACCAUGGAAAUAUTT-3' and antisense, 5'-AUAUUUCCAUGGUAGAUGCTT-3'; and negative control siRNA sense, 5'-UUCUCCGAACGUGUCACGUTT-3' and antisense, 5'-ACGUGACACGUUCGGAGAATT-3'. Cells were transfected with siRNAs (200 nM) or negative control siRNA (200 nM), using Lipofectamine® 2000 reagent (Invitrogen; Thermo Fisher Scientific, Inc.) for 72 h at 37˚C prior to reagent treatment.

Western blotting. Samples were homogenized in RIPA buffer (cat. no. KGP702-100; Changchun Keygen Biological Products Co., Ltd.) containing protease inhibitor at 4˚C, and then centrifuged at 16,000 x g for 15 min at 4˚C to extract soluble protein. Protein extracts were quantified using the Bradford method and loaded on 8 or 12% SDS-gels (20 μg per lane), resolved using SDS-PAGE, and then transferred to nitrocellulose membranes. Following blocking (5% skim milk) for 2 h at room temperature, membranes were incubated overnight at 4˚C with primary antibodies against CLC-7 (1:500), p-mTOR (1:1,000), mTOR (1:800), LC3 (1:2,000), p62 (1:1,000), ATG5 (1:800), Beclin1 (1:800), cathepsin D (1:1,000) or α-tubulin (1:2,000). Subsequently, the membranes were incubated with HRP-conjugated anti-rabbit secondary antibody (1:5,000) at room temperature for 2 h. Signals were visualized using a Quantity One system image analyzer (Bio-Rad Laboratories, Inc.) and densitometry analysis was performed using imaging software (Quantity One 4.6.2; Bio-Rad Laboratories, Inc.).

Immunofluorescence analysis. The samples were primary cardiomyocytes cultured on thin glass sheets. Immunofluorescence staining was performed as described previously (6,29). Each sample was rinsed four times (5 min each time) at room temperature with 0.01 M PBS before incubation with antibodies. Samples were fixed with 4% paraformaldehyde for 15 min at room temperature. Blocking was performed by immersing samples in 3% BSA (Sigma-Aldrich; Merck KGaA) for 1 h at room temperature. The primary antibodies used were rabbit anti-CLC-7 (1:100) and rat anti-LAMP1 (1:500). The samples were incubated with primary antibodies at 4˚C overnight, washed in PBS and incubated with secondary antibodies for 1 h at room temperature. The secondary antibodies used were goat polyclonal secondary antibody to rat IgG H&L (Alexa Fluor 488) (1:500; cat. no. ab150157; Abcam) or goat polyclonal secondary antibody to rabbit IgG H&L (Alexa Fluor 633) (1:100; cat. no. A-21070; Thermo Fisher Scientific, Inc.). Nuclei were stained with DAPI (1:200) for 2 min at room temperature. The quantification of co-localization was performed as described previously (33). Briefly, co-localization levels were quantified by measuring the intensity of regions where red and green fluorescence overlapped, using confocal software (LAS AF Lite 2.4.1; Leica Microsystems CMS GmbH) and ImageJ version 1.8.0 (National Institutes of Health). Co-localization was identified when the maxima of two overlapping peaks were shifted <20 nm. To assess lysosome-autophagosome fusion, primary antibodies against LC3B (1:200) and LAMP1 (1:500) were utilized (34). LAMP1 localizes in the outer membrane of lysosomes, whereas LC3B localizes in both the outer or inner membranes of autophagosomes (35). Therefore, double-positive LC3 and LAMP1 (yellow) puncta are used to evaluate lysosome-autophagosome fusion (34). All samples were viewed under a Leica TCS SP5 laser confocal scanning microscope (magnification, x600; Leica Microsystems GmbH), at the same voltage (220 V) to ensure comparability of fluorescence intensity. Every image was captured at a single confocal plane. In each group of samples, three fields of view were chosen randomly, all cells in each field were observed and quantified.

RT-qPCR. After removing medium, cell samples were immersed in RNAlater™ Solution and RNA was extracted using TRIzol® reagent. cDNA was synthesized using a QuantiNova™ reverse transcription kit according to the manufacturer's protocol. The reaction system was as follows: 50˚C for 15 min, 85˚C for 5 sec. Using QuantiNova™ SYBR® Green PCR kit, qPCR was performed on an Applied Biosystems® 7500 Real-Time PCR system (Applied Biosystems; Thermo Fisher Scientific, Inc.). The reaction conditions were as follows: 95˚C for 30 sec; 40 cycles of 95˚C for 10 sec and 60˚C for 30 sec; 95˚C for 15 sec, 60˚C for 60 sec, 95˚C for 15 sec. The sequences of the primers used were: LC3, forward, 5'-CTGCCTGTCCTGGAT AAGACCA-3' and reverse, 5'-CTGGTTGACCAGCAGGAA GAAG-3'; and p62 forward, 5'-GCTCTTCGGAAGTCAGCA AACC-3' and reverse, 5'-GCAGTTTCCCGACTCCATCTG T-3'; and β-actin forward, 5'-CATGTACGTTGCTATCCA GGC-3' and reverse, 5'-CTCCTTAATGTCACGCACGAT-3'. The $2^{-\Delta\Delta Cq}$ method was used for data analysis (36).

Cell Counting Kit-8 (CCK-8) viability assay. The CCK-8 assay was performed following the manufacturer's instructions. Following treatment, medium in each well (96-well plate) was replaced with 100 μl medium containing 10 μl CCK-8 reagent (Gen-view Scientific, Inc.) and incubated at 37˚C for 4 h. Optical density was measured using an automatic microplate reader (Thermo Fisher Scientific, Inc.) at 450 nm.

Assessment of lactate dehydrogenase (LDH) leakage. The leakage of LDH was determined using a CytoTox-ONETM Homogeneous Membrane Integrity assay (Promega Corporation). Briefly, 100 μl reaction buffer was transferred to each well (96-well plate) and the samples were incubated at room temperature for 15 min, then 25 μl stop buffer was added. The plates were shaken for 10 sec and the fluorescence intensity was measured at 560/580 nm. The reported data are given in percentages of the results of the respective control groups.

Lysosomal acidification assay. Lysosomal acidification was measured using LysoTracker and LysoSensor Probes (Thermo Fisher Scientific, Inc.) according to the manufacturer's protocol. The probe stock solution was diluted to a working concentration (LysoTracker, 50 nM; LysoSensor, 1 μM) in the medium. Cardiomyocytes were cultured in medium containing the probe for 1 h at 37˚C. The loading solution was replaced with fresh medium and cardiomyocytes were observed under a Leica TCS SP5 laser confocal scanning microscope (magnification, x600).

Transmission electron microscopy (TEM). TEM was used to detect autolysosomes or autophagosomes in cardiomyocytes. Briefly, freshly prepared samples were fixed overnight at 4˚C with 2.5% glutaraldehyde in 0.1 M phosphate buffer (pH 7.4) and 1% osmium tetroxide (pH 7.4). Samples were dehydrated with a series of acetone (90 and 100%) solutions and embedded in Epon (4 h) at room temperature. Before TEM, thin sections (60 nm) were cut and double-stained at room temperature with uranyl acetate (20 min) and lead citrate (5 min). Samples were viewed and imaged (indicated magnification, 80 kx) using a Philips TECNAI10 electron microscope (Philips Medical Systems, Inc.).

Statistical analysis. SPSS version 13.0 (SPSS, Inc.) was used for statistical analysis. Data are presented as the mean ± standard deviation of ≥3 independent repeats. An unpaired Student's t-test or one-way ANOVA with Bonferroni's post-test was used to compare differences between groups, based on the number of groups. $P<0.05$ was considered to indicate a statistically significant difference.

Results

Rapamycin treatment activates autophagy in the myocytes. Rapamycin is widely used in autophagy research (37,38). To establish a stable cell autophagy model, cardiomyocytes were treated with rapamycin, and the expression levels of autophagy-related proteins were detected. DMSO is an effective solvent for rapamycin (39); thus, DMSO groups, serving as control (vehicle) groups, were studied in parallel to rapamycin-treated groups. Following treatment with rapamycin for different periods of time (1, 3 and 6 h), p-mTOR/mTOR ratio was decreased ($P<0.05$ and $P<0.01$; Fig. 1A and B), suggesting functional inhibition of mTOR. Moreover, the increase in the expression levels of autophagy-related proteins, including Beclin1, ATG5 and LC3 further confirmed activation of autophagy ($P<0.05$ and $P<0.01$; Fig. 1A and B).

To observe autophagy more directly, following rapamycin treatment for 6 h, immunofluorescence staining was performed (Fig. 1F and G). The number of autophagosomes (green) was significantly increased ($P<0.001$), in line with the higher number of autolysosomes (yellow, $P<0.001$). Additionally, total autophagosome and autolysosome counts suggested enhanced autophagy ($P<0.01$).

Lysosomes serve pivotal roles in autophagy, and their acidification level is also an important indicator of autophagy (19). In the present study, following rapamycin treatment, the increase in green fluorescence intensity suggested that rapamycin treatment activated lysosomal function ($P<0.0001$; Fig. 1C and D). Cathepsin D, a lysosomal protease, is stable at low pH levels, and indirectly reflects lysosomal acidity (40). Following 3 and 6 h of rapamycin treatment, an increase in the protein expression levels of cathepsin D was observed ($P<0.05$; Fig. 1A and B), further suggesting that rapamycin enhanced lysosomal function.

To investigate the effects of autophagy on cell status, cardiomyocyte viability was assessed using CCK-8 and LDH assays. The results demonstrated that rapamycin did not significantly affect cell viability in early autophagy (within 6 h) under normal conditions (Fig. 1E). Taken together, the results suggested that rapamycin treatment activated autophagy in cardiomyocytes.

Lysosomal acidification promotes myocardial autophagy. Since enhanced autophagy and activated lysosomal acidification were observed following rapamycin treatment, the role of lysosomes in cardiomyocyte autophagy was further examined (Fig. 2A-I). CQ, a lysosomal acidification inhibitor (41) was used to pretreat cardiomyocytes before rapamycin treatment and autophagy was monitored. Cathepsin D protein expression was reduced following CQ treatment ($P<0.01$; Fig. 2A and B), which was in line with the changes in lysosomal green fluorescence intensity ($P<0.01$; Fig. 2D and E). These findings suggest that lysosomal acidification was inhibited by CQ. Along with decreased lysosomal acidification, the LC3II and p62 expression levels were increased ($P<0.01$; Fig. 2A and C). The increase in LC3II and p62 expression levels may have been due to increased production or reduced degradation; thus, the mRNA expression levels were assessed. No significant changes in mRNA expression levels following CQ treatment were observed, eliminating the possibility of gene expression variations (Fig. 2F). These results indicated that lysosomal weakening of acidification induced autophagosome accumulation and obstructed autophagy.

Immunofluorescence results further confirmed these findings (Fig. 2H and I). The proportion of uncombined autophagosomes (green; $P<0.001$) and lysosomes (red; $P<0.01$) was increased, while the proportion of autolysosomes was decreased (yellow; $P<0.01$) following CQ treatment, suggesting reduced autophagosome-lysosome fusion and accumulation of autophagy substrates. The significant increase in the total amount of autophagosomes and autolysosomes ($P<0.05$) also indicated enhanced substrate accumulation. Additionally, cardiomyocyte viability was decreased following CQ treatment, as shown in the CCK-8 and LDH assays ($P<0.01$; Fig. 2G).

The aforementioned results demonstrated that insufficient lysosomal function results in autophagosome accumulation and cardiomyocyte damage, indicating that lysosomal acidification is crucial for functional cardiomyocyte autophagy.

CLC-7 is recruited to lysosomes during cardiomyocyte autophagy. Subsequently, changes in CLC-7 expression were determined using western blotting (Fig. 3A and B). There was a slight, but insignificant increase in CLC-7 expression following rapamycin treatment. Results of the immunofluorescence analysis also showed similar results (Fig. 3C and D).

Extensive lysosomal recruitment of CLC-7 in rapamycin-treated groups was observed (Fig. 3E-H). LAMP1 was used as the marker of lysosomes (27). CLC-7 co-localization with LAMP-1 was increased in the rapamycin-treated groups compared with the DMSO group. In the DMSO group, CLC-7 was distributed diffusely throughout the cytosol. There was either partial or no co-localization between the two proteins. By contrast, in the rapamycin-treated groups, CLC-7 localized to the perinuclear region and was concentrated in lysosomes (Fig. 3E). Co-localization levels were quantified by measuring red and green fluorescence intensity overlaps, as described previously (33). Complete co-localization was observed when the maxima of two overlapping peaks were shifted <20 nm.

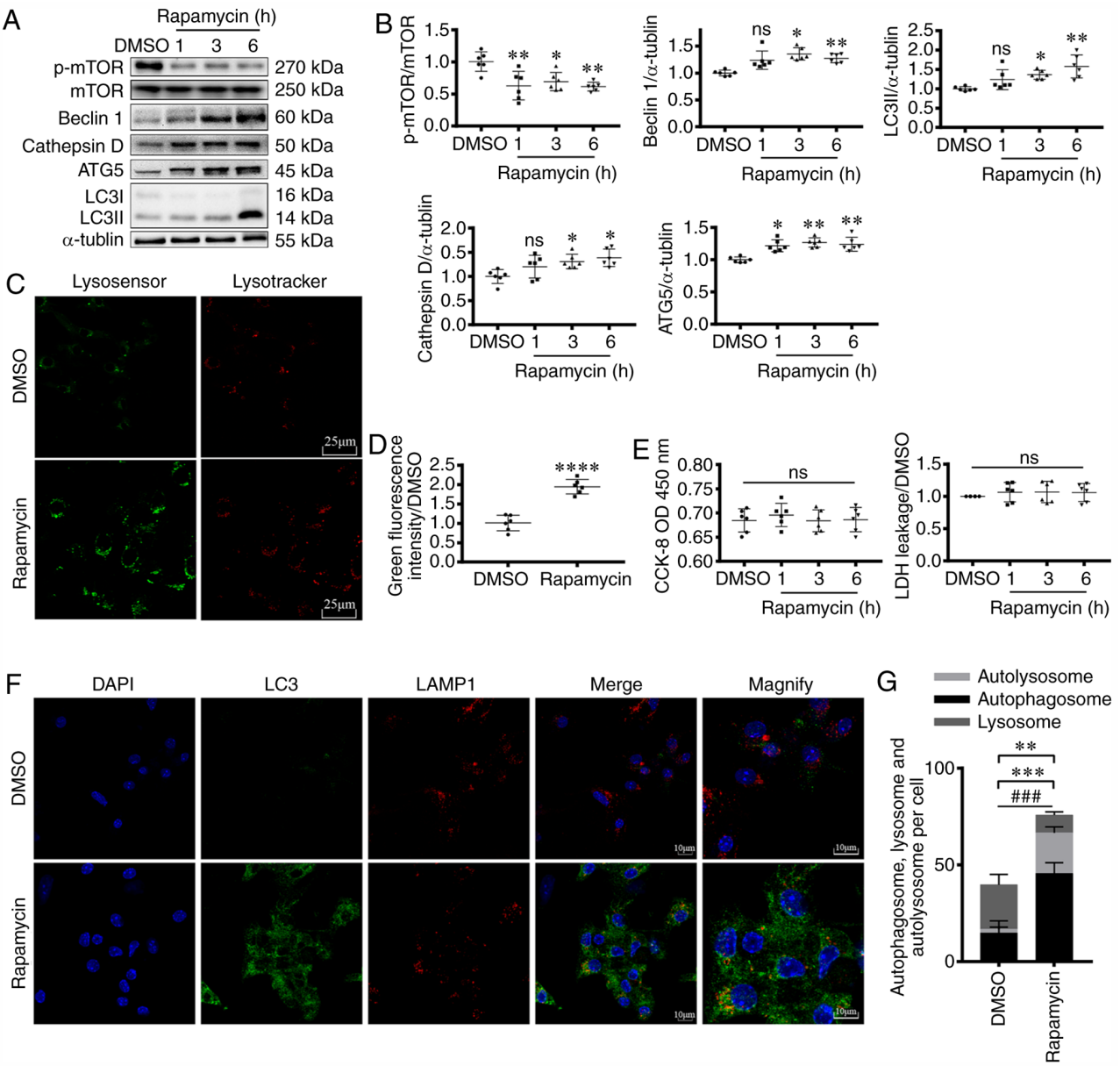

Figure 1. Rapamycin treatment activates myocardial autophagy pathway. (A and B) Western blotting, (C, D, F and G) fluorescence staining and (E) CCK-8 and LDH analyses showing the induction of myocardial autophagy following rapamycin treatment. (A) Western blotting was used to assess p-mTOR (270 kDa), mTOR (250 kDa), Beclin1 (60 kDa), Cathepsin D (50 kDa), ATG5 (45 kDa) and LC3 (I: 16 kDa, II: 14 kDa) expression levels in cardiomyocytes following rapamycin treatment for 1, 3 or 6 h. α-tubulin (55 kDa) levels were measured as the loading control. (B) Graphs representing the results. ANOVA. *P<0.05, **P<0.01 vs. DMSO group. n=6. (C) Lysosomal acidification in the absence (DMSO) or presence of 200 nM rapamycin (6 h) were measured using LysoTracker and LysoSensor. Indicators show pH-dependent increase of green fluorescence intensity upon lysosomal acidification. (D) Quantification of results. Scale bar, 25 μm. Unpaired t-test. ****P<0.0001 vs. DMSO. n=6. (E) CCK-8 and LDH analysis of cardiomyocyte viability following rapamycin treatment. ANOVA. n=6. (F) Confocal images of LC3^{+} puncta (green dots) and LAMP1^{+} puncta (red dots) in cardiomyocytes. (G) Graph demonstrates the mean number of autolysosomes (yellow dots) and autophagosomes (green dots). Scale bar, 10 μm. Unpaired t-test. **P<0.01 vs. DMSO, comparing the number of autolysosome + autophagosome; ***P<0.001 vs. DMSO, comparing the number of autolysosome; $^{###}$P<0.001 vs. DMSO, comparing the number of autophagosome. n=5. CCK-8, Cell Counting Kit-8; LDH, lactate dehydrogenase; p-phospho-; ns, not significant; ATG5, autophagy related 5; LC3, microtubule associated protein 1 light chain 3; LAMP1, lysosomal-associated membrane protein 1; OD, optical density.

An increase in overlapping of fluorescence intensity peaks was observed in rapamycin-treated groups compared with the DMSO groups (P<0.01; Fig. 3F-G). These findings suggested that there was increase in intracellular CLC-7 located in the lysosomes following rapamycin treatment. Thus, CLC-7 protein expression in the lysosomes in the perinuclear region was subsequently observed (Fig. 3H). In rapamycin-treated groups, increased CLC-7-lysosome co-localization (yellow) was observed, in which the green puncta fused with the red puncta completely. By contrast, in the DMSO groups, partial co-localization was viewed, and various green puncta were distributed besides the red puncta. Together, these findings suggested that CLC-7 was recruited to lysosomes during cardiomyocyte autophagy.

Autophagy substrates accumulate following CLC-7 silencing. As enhanced CLC-7-LAMP1 co-localization was observed following rapamycin treatment, it was hypothesized that

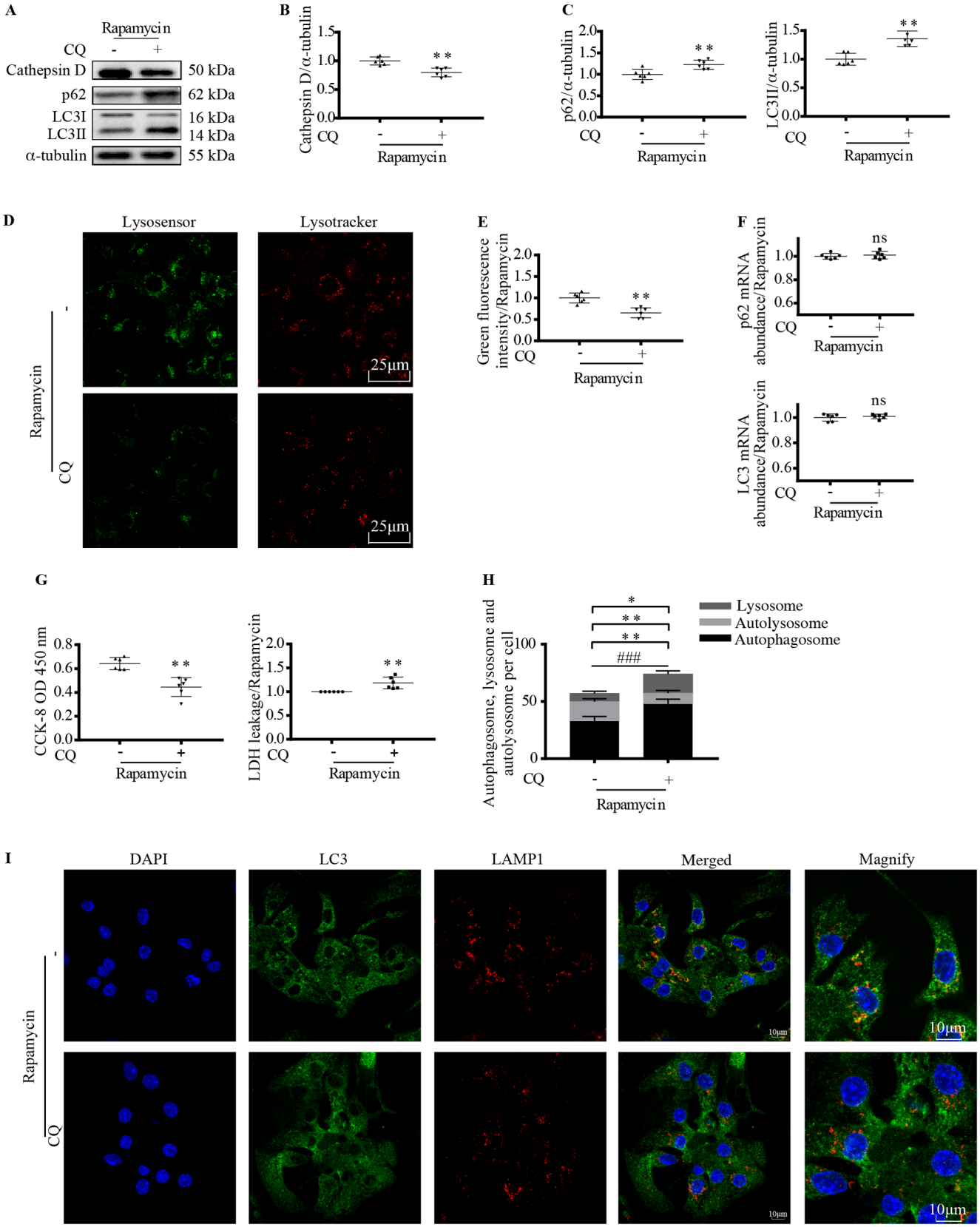

Figure 2. Lysosomal acidification promotes myocardial autophagy. Cardiomyocytes were treated with 200 nM rapamycin for 6 h with or without pretreatment with CQ (100 nM for 2 h). (A) Western blotting and semi-quantitative analysis of (B) cathepsin D, (C) LC3II and p62 protein expression levels. Unpaired t-test. **P<0.01 vs. untreated control. n=6. (D) Lysosomal acidification was measured using LysoTracker and LysoSensor. (E) Graph shows quantification of green fluorescence intensity. Scale bar, 25 μm. Unpaired t-test. **P<0.01 vs. untreated control. n=6. (F) Analysis of LC3 and p62 gene expression levels using reverse transcription-quantitative PCR. Unpaired t-test. n=6. (G) Cardiomyocyte viability was evaluated using a CCK-8 and LDH assay. Unpaired t-test. **P<0.01 vs. untreated control. n=6. (H) Mean number of autolysosomes (yellow dots) and autophagosomes (green dots) were quantified. (I) Confocal images show LC3 co-localization with LAMP1. Scale bar, 10 μm. Unpaired t-test. *P<0.05, autolysosome + autophagosome; **P<0.01, lysosome, autolysosome; $^{\#\#\#}$P<0.001, autophagosome. n=5. CQ, chloroquine; LC3, microtubule associated protein 1 light chain 3; CCK-8, Cell Counting Kit-8; LDH, lactate dehydrogenase; LAMP1, lysosomal-associated membrane protein 1; ns, not significant; OD, optical density.

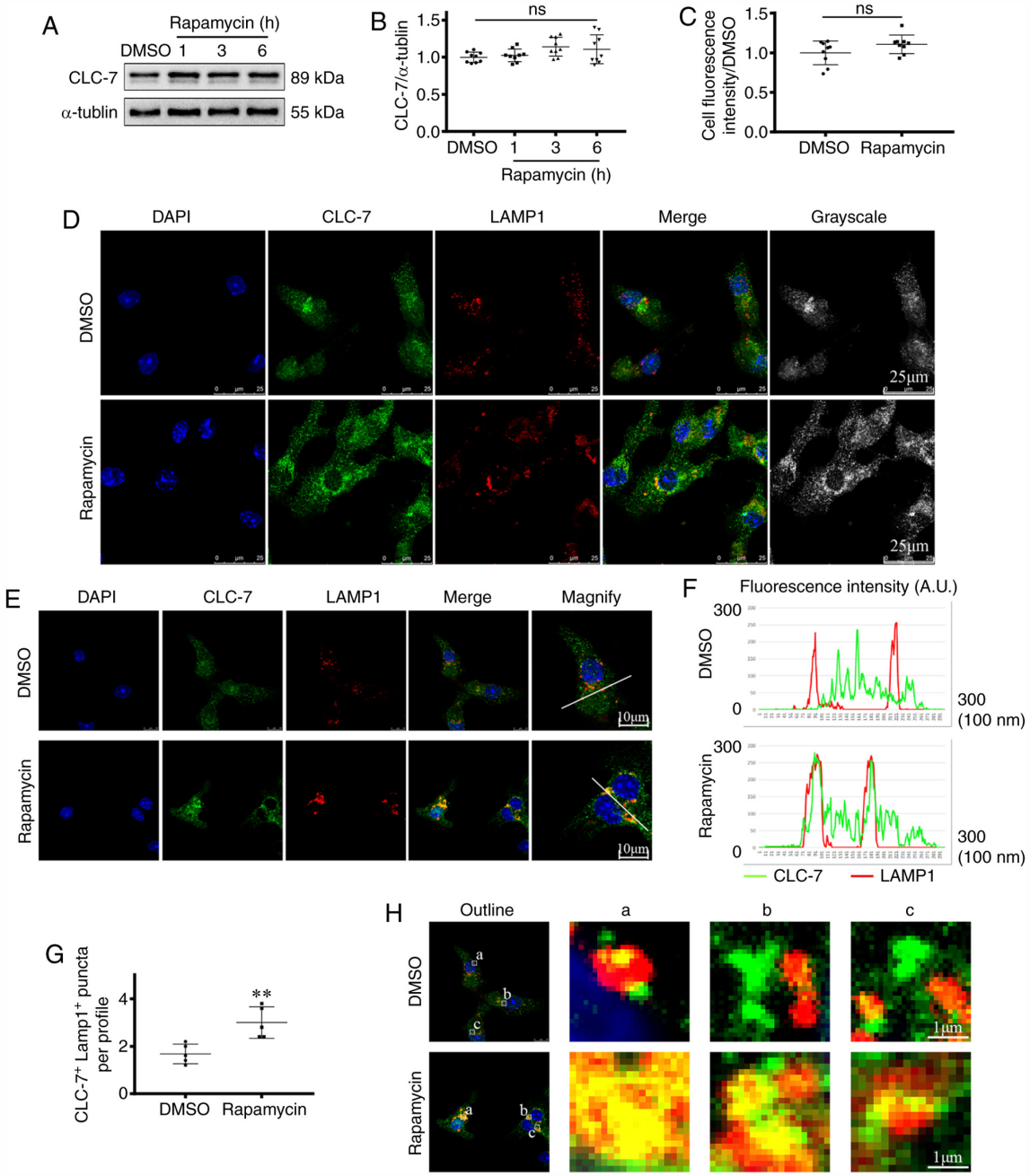

Figure 3. CLC-7 is recruited to lysosomes during cardiomyocyte autophagy (A and B) Western blotting and (C-H) fluorescence staining showing myocardial CLC-7 protein expression levels and localization following rapamycin treatment. Immunofluorescent confocal micrographs of cardiomyocytes stained for anti-CLC-7 (green), anti-LAMP1 (red) and DAPI for the nuclei (blue). (A) Protein expression levels of CLC-7 were detected by western blotting and (B) semi-quantified. ANOVA, n=9. (C) Quantitative fluorescence analysis of total CLC-7, as detecting by (D) immunofluorescent staining. Scale bar, 25 μm. Unpaired t-test. n=9. (E) Amplified views show co-localization levels of CLC-7 and LAMP1. Scale bar, 10 μm. (F) The graph shows the fluorescence intensity peaks along profiles crossing CLC-7$^+$ LAMP1$^+$ puncta indicated in magnified micrograph in panel (E). (G) Co-localization levels were quantified by measuring fluorescence intensity overlaps, using confocal software. Unpaired t-test. **P<0.01 vs. DMSO group. n=5. (H) Lysosomes in the perinuclear region were viewed and shown in magnified images a, b and c. Scale bar, 1 μm. LAMP1, lysosomal-associated membrane protein 1; CLC-7, H(+)/Cl(-) exchange transporter 7; ns, not significant.

CLC-7 may participate in lysosomal acidification and autolysosome digestion. Therefore, CLC-7 expression was knocked down using CLC-7 siRNAs (Si1 and Si2). Following siRNA transfection, CLC-7 protein expression levels were significantly decreased as detected via western blotting (P<0.01; Figs. 4A, B, D, F and S1) and immunofluorescence observation (P<0.05; Fig. 4G and H). Along with decreased cellular CLC-7 levels, deficient CLC-7-lysosome co-localization was also observed (Fig. 4H).

Immunoblotting results demonstrated that CLC-7 was involved in autophagy (Fig. 4A and B). Moreover, following rapamycin treatment, LC3II and p62 expression levels were increased in the siRNA-transfected groups, suggesting accumulation of autophagy substrates (P<0.05; Fig. 4A and B). To investigate the effect of CLC-7 on substrate generation or digestion, gene expression levels of LC3 and p62 were assessed. However, increased LC3 and p62 protein levels were not associated with increased transcription (Fig. 4E).

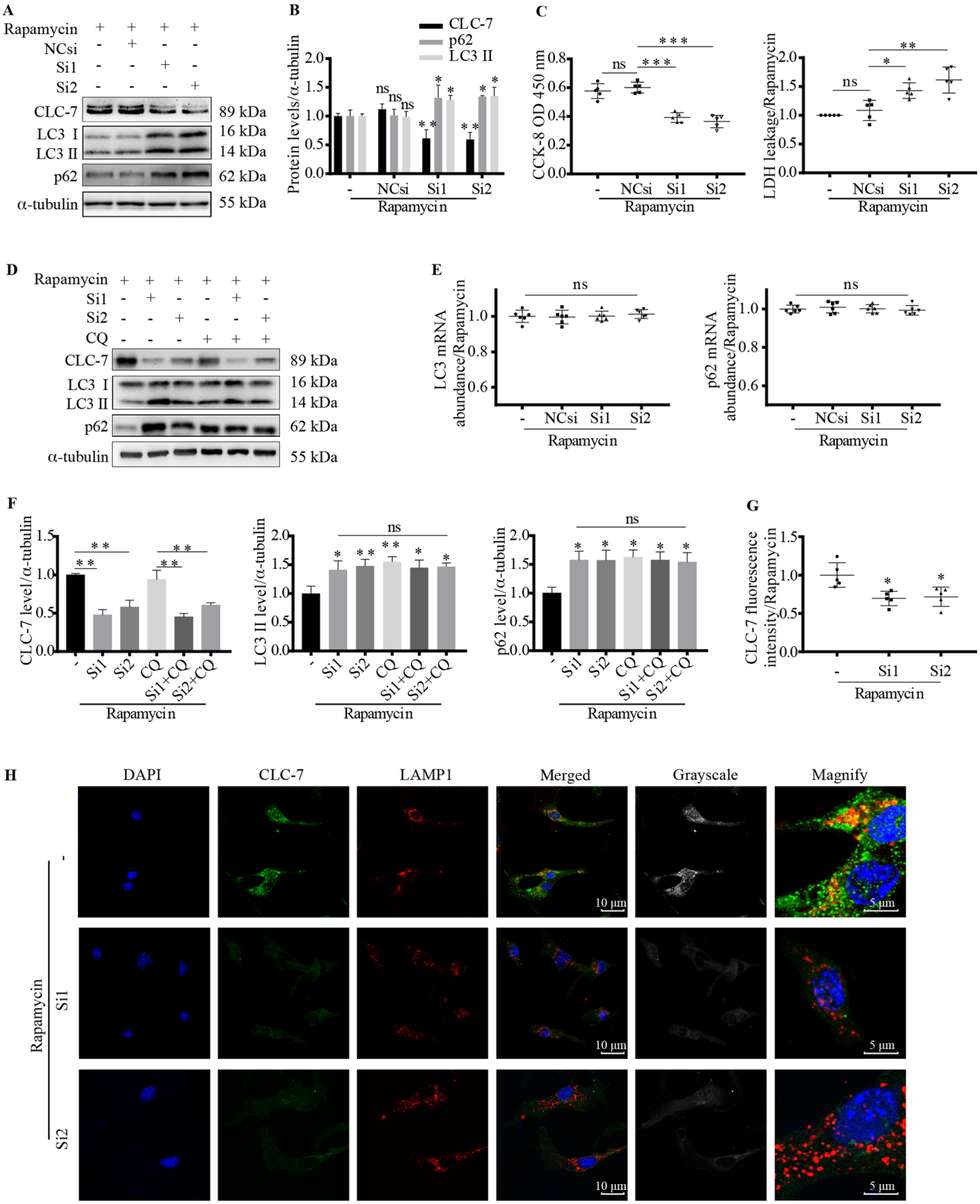

Figure 4. Autophagy substrates accumulate following CLC-7 silencing. (A, B, D and F) Expression levels of autophagy-related proteins and CLC-7 were measured using western blotting, (E) RT-qPCR and (G and H) immunofluorescence. (C) Cell viability was assessed using CCK-8 and LDH assays following transfection with CLC-7 siRNAs with or without CQ pretreatment. (A) Western blot analysis of (B) expression levels of autophagy-related proteins following transfection with CLC-7 siRNAs or NCsi. *P<0.05, **P<0.01 vs. NCsi group. n=3. (C) Cardiomyocyte viability analysis using CCK-8 and LDH assays. *P<0.05, **P<0.01, ***P<0.001. n=5. (D) Western blot analysis of (F) expression levels of autophagy-related proteins following transfection with CLC-7 siRNAs with or without CQ (100 nM for 2 h) pretreatment. *P<0.05, **P<0.01 vs. untreated control. n=3. (E) LC3 and p62 mRNA expression levels were assessed using RT-qPCR. ANOVA, n=6. (G) Quantification of (H) immunofluorescence analysis of the localization and protein expression levels of CLC-7 following transfection with CLC-7 siRNAs. Scale bar, 5 or 10 μm. ANOVA. *P<0.05 vs. untreated control. n=5. CLC-7, H(+)/Cl(-) exchange transporter 7; siRNA, small interfering RNA; CQ, chloroquine; CCK-8, Cell Counting Kit-8; LDH, lactate dehydrogenase; NCsi, negative control siRNA; LC3, microtubule associated protein 1 light chain 3; RT-qPCR, reverse transcription-quantitative PCR; ns, not significant; OD, optical density.

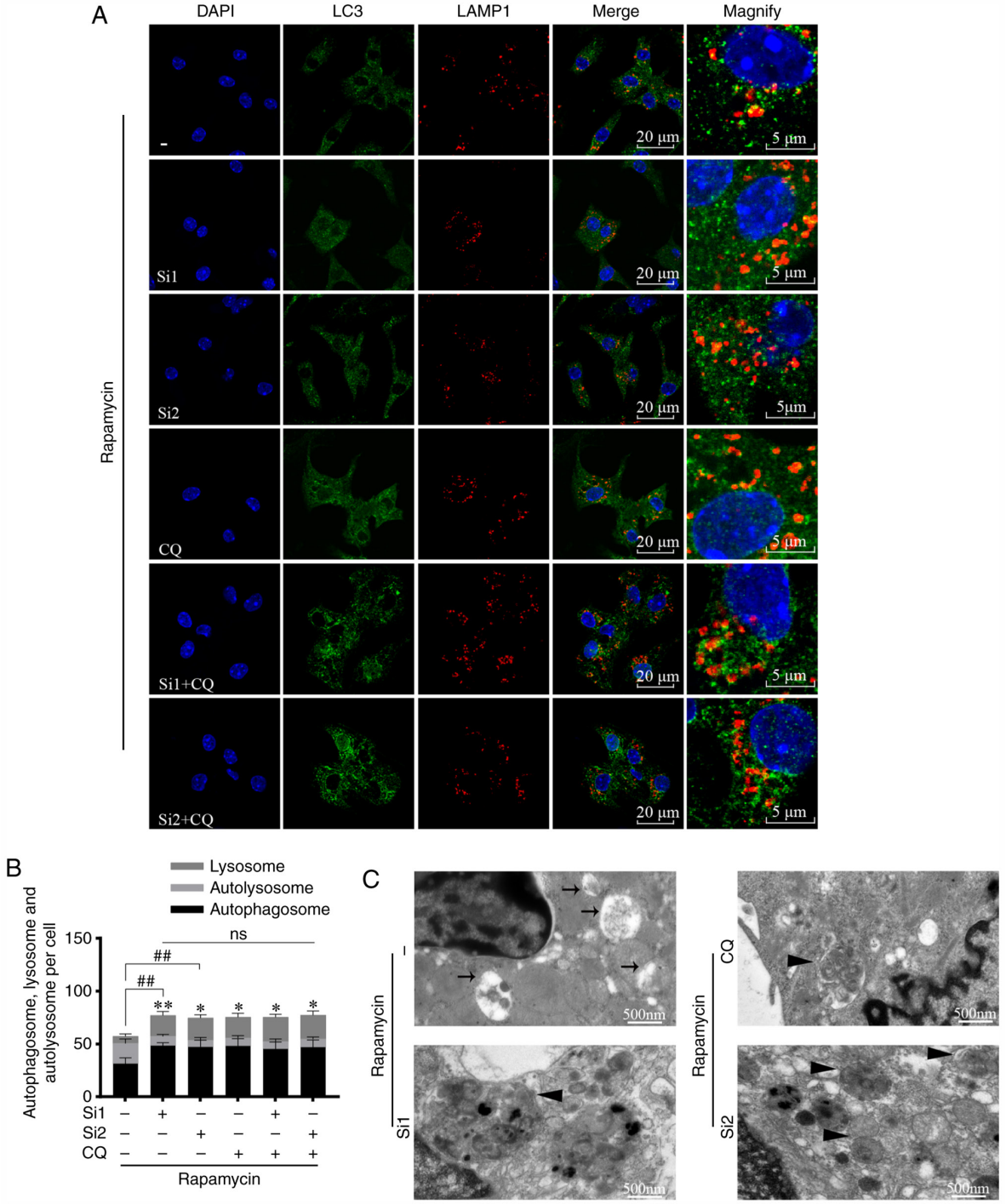

Figure 5. CLC-7 silencing causes autophagosome accumulation. Cardiomyocytes were transfected with 200 nM CLC-7 siRNAs or pretreated with 100 nM CQ for 2 h, then treated with 200 nM rapamycin for 6 h. (A) Cardiomyocytes were incubated with antibodies against LC3 (green) and LAMP1 (red) and viewed via confocal microscopy. Scale bar, 5 μm. (B) Quantitative results are shown in the bar chart. Autolysosomes (yellow dots) and autophagosomes (green dots) were counted per cell in three microscopic fields per group. The mean number was calculated. ANOVA. *P<0.05, **P<0.01, autolysosome; $^{\#\#}$P<0.01, autophagosome. n=5. (C) Electron micrograph showing the morphology of autophagosomes and autolysosomes in cardiomyocytes; triangles represent autophagosomes, arrows represent autolysosomes. Scale bar, 500 nm. Independent experiments were repeated three times. CLC-7, H(+)/Cl(-) exchange transporter 7; siRNA, small interfering RNA; NCsi, negative control siRNA; LC3, microtubule associated protein 1 light chain 3; LAMP1, lysosomal-associated membrane protein 1; CQ, chloroquine; ns, not significant.

CQ, the lysosomal function inhibitor, was used to further determine the target of CLC-7. CLC-7 knockdown increased LC3 II and p62 protein levels (P<0.05 and P<0.01; Fig. 4F), but there was no further increase when cells were additionally treated with CQ. Cell viability was measured using CCK-8 and LDH assays. Following rapamycin treatment, CLC-7 knockdown decrease cardiomyocyte viability (P<0.05, P<0.01 and P<0.001; Fig. 4C), suggesting CLC-7 may be important for cardiomyocyte survival and was involved in autophagy.

CLC-7 knockdown decreased the co-localization of LC3 (green) and LAMP1 (red) (Fig. 5A and B). In CLC-7-knockdown cells, the proportion of uncombined autophagosomes increased

(P<0.01), whereas the proportion of autolysosomes (yellow) decreased (P<0.05 and P<0.01). These trends were not further altered when cells were additionally treated with CQ (Fig. 5B). These findings suggested that CLC-7 knockdown blocked autophagy, and lysosomes served as the primary targets. Furthermore, the ultrastructure was observed via TEM (Fig. 5C). Following rapamycin treatment (6 h), in control groups, there was an increase in digested autophagy substrates visible in autolysosomes (black arrow), and an increase in undigested organelles within the lumina (black triangle) following CLC-7 knockdown or CQ treatment. The results indicated that CLC-7 knockdown impaired autophagy substrate clearance.

CLC-7 silencing results in decreased lysosomal acidification. Since CLC-7 knockdown and CQ treatment appeared to exhibit a partial same effect on autophagy, the role of CLC-7 in lysosomes, specifically on lysosomal acidification, was assessed using LysoTracker and LysoSensor Probes. The green fluorescence levels were decreased in CLC-7 siRNA-transfected cells, irrespective of CQ treatment (P<0.05 and P<0.01; Fig. 6A and B). The difference between transfected cells treated with or without CQ was not significant. These findings indicated that lysosomal acidification was weakened in the CLC-7 siRNA transfected cells, and CQ did not have further effect on acidification in the knockdown cells. Changes in cathepsin D protein expression levels also provided similar results (P<0.01; Fig. 6C and D), suggesting weak lysosomal acidification. Collectively, the results suggested that CLC-7 promoted lysosomal acidification in autophagy in cardiomyocytes.

Discussion

The present study demonstrated that CLC-7 was recruited to lysosomes in cardiomyocytes during autophagy. CLC-7 knockdown attenuated lysosomal acidification, thereby blocking autolysosome self-degradation. These findings suggested that CLC-7 participated in the regulation of myocardial lysosomal acidification-mediated autophagy. Furthermore, in previous studies (23,24,27), the pathological changes of CLC-7 were examined in chronic diseases, whereas, to the best of our knowledge, there are no studies on the role of CLC-7 in autophagy. The present study provided evidence that antiporters may serve a more pronounced role during early autophagy. Autophagy occurs under various acute stress responses, such as hypoxia, ischemia and oxidative stress (1). This indicates that the role of CLC7 should be evaluated in both relatively protracted or genetic diseases, but also in certain conditions associated with acute stress.

Studies have confirmed that CLC-7 is located in the endoplasmic reticulum in the perinuclear region or is diffused in the cytoplasm in an inactivated state, and transferred to lysosomes where it becomes functionally activated (25,26). Inefficient CLC-7 delivery to lysosomes aggravates Alzheimer's disease (26), while aberrant CLC-7 function leads to osteoarthritis (42). In the present study, lysosomal recruitment of CLC-7 was increased following activation of autophagy in mouse cardiomyocytes. In inactivated autophagic vesicles, increased diffuse staining of CLC-7 in cardiomyocytes was observed, dissimilar to the punctate LAMP1 positive staining seen in the activated autophagic vesicles. These results suggested that CLC-7 was involved in the regulation of autophagy.

In the present study, autophagy was induced using rapamycin, a specific mTOR inhibitor, as has been performed previously (37). mTOR is the initial switch for activation of autophagy (43). In this study, p-mTOR/mTOR was decreased, while as the expression levels of autophagy-related proteins were increased following rapamycin treatment. These findings demonstrated that autophagy was induced. Additionally, CLC-7 localization changed following induction of autophagy. However, autophagy is an intricately connected process that is involved in numerous complex conditions (1), and whether CLC-7 alone underlies the aberrant autophagy in these pathological conditions requires further investigation.

Lysosomes are key components in autophagy flux (44). In the present study, acid-sensitive lysosomal tracker and cathepsin D were used to detect lysosomal acidification. P62, an autophagy receptor, is a marker reflecting autophagy levels, and its aggregation indicates autophagosome accumulation (12,41,45). LC3II, which is formed following cleavage of LC3I, is located on autophagosome membranes during autophagy. Therefore, the levels of LC3II are used as autophagy detecting tools (40,45). Following inhibition of lysosomal acidification using CQ, lysosomal acidification decreased and substrate LC3II and p62 protein expression levels increased, suggesting autophagosome accumulation. Thus, the present results demonstrated that lysosomal acidification promoted autophagy substrate degradation; a finding that is in line with previous studies (14,37,44).

LAMP1 is considered a lysosomal marker protein, and as the autophagosomes fuse with lysosomes, LC3 and LAMP1 co-localized puncta are detectable in autolysosomes (40). In the present study, CQ treatment was used as a positive control for blocking autophagy flux. CQ disrupts autophagy by inhibiting lysosomal acidification (37). A previous study reported that rapamycin activated autophagy and autophagosome-lysosome fusion in CHO cells, whereas CQ increased lysosomal pH, and therefore blocked the fusion (37). In the present study, autophagosome-lysosome fusion was increased following rapamycin treatment and was decreased after additional treatment with CQ. CLC-7 silencing or CQ treatment reduced the number of $LC3^{+}$ $LAMP1^{+}$ puncta, whereas the number of $LC3^{+}$ puncta increased, suggesting decreased autophagosome-lysosome fusion and an accumulation of unfused autophagosomes. Furthermore, the difference between the counts of autophagosomes, and the abundance of LC3 and p62 mRNA expression levels in the two treatment conditions was insignificant, indicating a similarity in the effect of CLC-7 knockdown and CQ treatment on autophagy. CQ did not further increase the of autophagy substrates, which were accumulated after CLC-7 silencing. Accumulation of the substrates was observed in the autophagosomes following CLC-7 knockdown or CQ treatment using TEM. These results further support our previous hypothesis that CLC-7 knockdown and CQ treatment have similar effect on autophagy. Lysosomal acidification was inhibited by CLC-7 knockdown, suggesting that lysosomal acidification was the target, and CLC-7 silencing interfered with autolysosome-mediated degradation by blocking lysosomal acidification. Previous studies have revealed that v-ATPase in lysosome membrane

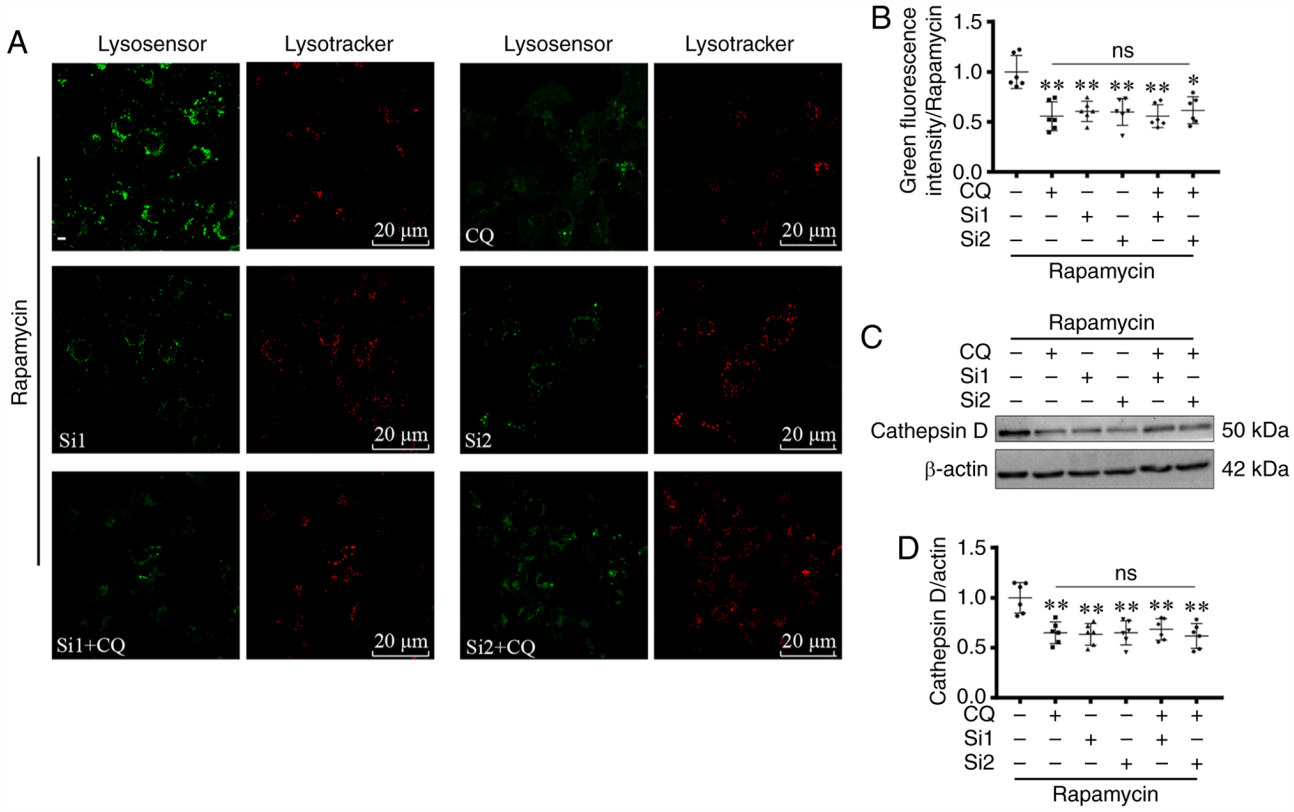

Figure 6. CLC-7 silencing results in weak lysosomal acidification. Cardiomyocytes were transfected with CLC-7 siRNA or pretreated with 100 nM CQ for 2 h, and then treated with 200 nM rapamycin for 6 h. (A) Lysosomal acidification was assessed using lysosomal probes. Scale bar, 20 μm. (B) Relative green fluorescence was quantified. ANOVA. *P<0.05, **P<0.01 vs. untreated control. n=6. (C) Cathepsin D protein expression levels were detected using western blotting and (D) semi-quantified. ANOVA. **P<0.01 vs. untreated control. n=6. CLC-7, H(+)/Cl(-) exchange transporter 7; CQ, chloroquine; siRNA, small interfering RNA; NCsi, negative control siRNA; ns, not significant.

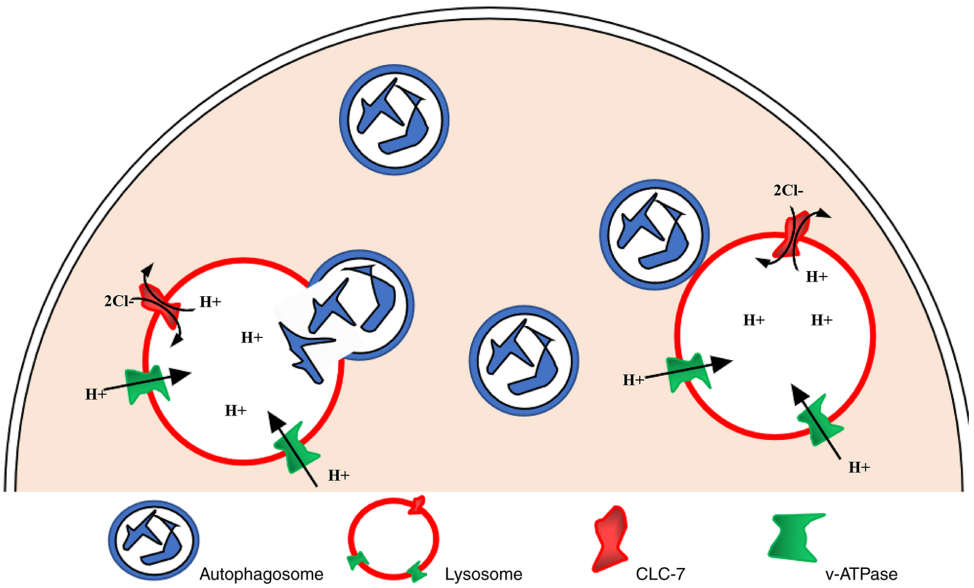

Figure 7. Schematic depiction of CLC-7-associated lysosomal acidification and autophagosome degradation. CLC-7, H(+)/Cl(-) exchange transporter 7; v-ATPase, vacuolar-type H+-ATPase.

transfers H^+ into the lumen to acidify lysosomes (16,19,46) (as shown in the schematic diagram in Fig. 7). At the same time, the increase in potential caused by the continuous accumulation of luminal H^+ hinders the further transfer of H^+. CLC-7, as a $2Cl^-/1H^+$ antiporter, exports one H^+ and imports two Cl^-, resulting in a net negative charge to offset the increase in the luminal potential, thereby promoting the continuous flow of H+ and lysosomal acidification further (21,22).

However, the present study has the following limitations. Although it has been clarified that CLC-7 is indispensable for

autophagy flux, further investigation should be conducted. For instance, under stress conditions, such as oxidative stress or acute hypoxia, it should be examined whether impaired lysosomal acidification is caused by insufficient CLC-7 expression or dysfunction, or a joint involvement. Secondly, the specific molecular mechanism that causes insufficient CLC-7 expression or dysfunction under such stress conditions needs to be clarified in order to identify effective targets in improving lysosomal acidification and autophagy. It should also be considered that CLC-7, as a membrane protein, may directly participate in the molecular interaction in autophagosome-lysosome fusion. Additionally, CLC-7 ion transport function may require further investigation using electrophysiological techniques.

In conclusion, to the best of our knowledge, the present study was the first to examine the roles of CLC-7 in autophagy. The present results suggested that CLC-7 was essential for lysosomal acidification and lysosome-mediated autophagy in cardiomyocytes. These findings increase the understanding of CLC-7 function in autophagy, and provide a novel insight into the role of CLC-7, differing from that in CLC-7 deficiency-related diseases. CLC-7 activation may be a novel and valuable therapeutic target for improving autophagy. Additional studies may yield further insights into organ therapy following acute stress and in autophagy-mediated diseases.

Acknowledgements

Not applicable.

Funding

This work was supported by the Key Program of National Natural Science Foundation of China (grant no. 81430042).

Availability of data and materials

The datasets used and/or analyzed in the current study are available from the corresponding authors on reasonable request.

Authors' contributions

YH and DZ conceived the research and supervised the study. JL, JW and YL designed the experiments with help from DZ and XZ. JL and JW performed the experiments with help from XZ, QZ, RFY and JJ. JL, JW and CD participated in the acquisition of raw data and computed data and collated the data. JL, JW and XZ analyzed the data. JL, JW and CD wrote, edited and revised the manuscript. All authors participated in revising the manuscript. All authors read and approved the final manuscript.

Ethics approval and consent to participate

Animal-based investigations were designed in accordance with the Guide for the Care and Use of Laboratory Animals published by the National Institutes of Health (NIH Pub. No. 85-23, revised 1996). The present study was reviewed and approved by the Animal Experiment Ethics Committee of the Third Military Medical University in Chongqing, China. All experiments involving animals were performed in accordance with the ethical standards of the institution or practice at which the studies were performed.

Patient consent for publication

Not applicable.

Competing interests

The authors declare that they have no competing interests.

References

1. Ravanan P, Srikumar IF and Talwar P: Autophagy: The spotlight for cellular stress responses. Life Sci 188: 53-67, 2017.
2. Glick D, Barth S and Macleod KF: Autophagy: Cellular and molecular mechanisms. J Pathol 221: 3-12, 2010.
3. Deng M, Huang L and Zhong X: β-asarone modulates Beclin1, LC_3 and p62 expression to attenuate Abeta40 and Abeta42 levels in APP/PS1 transgenic mice with Alzheimer's disease. Mol Med Rep 21: 2095-2102, 2020.
4. Huang YS: Myocardial damage and its mechanism in burn patients. Zhonghua Zheng Xing Shao Shang Wai Ke Za Zhi 9: 99-102, 1993 (In Chinese).
5. Li Y, Ge S, Peng Y and Chen X: Inflammation and cardiac dysfunction during sepsis, muscular dystrophy, and myocarditis. Burns Trauma 1: 109-121, 2013.
6. Xiao R, Teng M, Zhang Q, Shi XH and Huang YS: Myocardial autophagy after severe burn in rats. PLoS One 7: e39488, 2012.
7. Matsui Y, Takagi H, Qu X, Abdellatif M, Sakoda H, Asano T, Levine B and Sadoshima J: Distinct roles of autophagy in the heart during ischemia and reperfusion: Roles of AMP-activated protein kinase and Beclin 1 in mediating autophagy. Circ Res 100: 914-922, 2007.
8. Troncoso R, Vicencio JM, Parra V, Nemchenko A, Kawashima Y, Del Campo A, Toro B, Battiprolu PK, Aranguiz P, Chiong M, *et al*: Energy-preserving effects of IGF-1 antagonize starvation-induced cardiac autophagy. Cardiovasc Res 93: 320-329, 2012.
9. Yan L, Vatner DE, Kim SJ, Ge H, Masurekar M, Massover WH, Yang G, Matsui Y, Sadoshima J and Vatner SF: Autophagy in chronically ischemic myocardium. Proc Natl Acad Sci USA 102: 13807-13812, 2005.
10. Huang YS: Autophagy and hypoxic ischemic myocardial damage after severe burn. Zhonghua Shao Shang Za Zhi 34: 3-7, 2018 (In Chinese).
11. Marino G, Niso-Santano M, Baehrecke EH and Kroemer G: Self-consumption: The interplay of autophagy and apoptosis. Nat Rev Mol Cell Biol 15: 81-94, 2014.
12. Oh JM, Choi EK, Carp RI and Kim YS: Oxidative stress impairs autophagic flux in prion protein-deficient hippocampal cells. Autophagy 8: 1448-1461, 2012.
13. Funakoshi-Hirose I, Aki T, Unuma K, Funakoshi T, Noritake K and Uemura K: Distinct effects of methamphetamine on autophagy-lysosome and ubiquitin-proteasome systems in HL-1 cultured mouse atrial cardiomyocytes. Toxicology 312: 74-82, 2013.
14. Gonzalez P, Mader I, Tchoghandjian A, Enzenmuller S, Cristofanon S, Basit F, Debatin KM and Fulda S: Impairment of lysosomal integrity by B10, a glycosylated derivative of betulinic acid, leads to lysosomal cell death and converts autophagy into a detrimental process. Cell Death Differ 19: 1337-1346, 2012.
15. Ma X, Liu H, Foyil SR, Godar RJ, Weinheimer CJ, Hill JA and Diwan A: Impaired autophagosome clearance contributes to cardiomyocyte death in ischemia/reperfusion injury. Circulation 125: 3170-3181, 2012.
16. Mindell JA: Lysosomal acidification mechanisms. Annu Rev Physiol 74: 69-86, 2012.
17. Decker RS and Wildenthal K: Lysosomal alterations in hypoxic and reoxygenated hearts. I. Ultrastructural and cytochemical changes. Am J Pathol 98: 425-444, 1980.
18. Weinert S, Jabs S, Supanchart C, Schweizer M, Gimber N, Richter M, Rademann J, Stauber T, Kornak U and Jentsch TJ: Lysosomal pathology and osteopetrosis upon loss of H+-driven lysosomal Cl-accumulation. Science 328: 1401-1403, 2010.

19. Ishida Y, Nayak S, Mindell JA and Grabe M: A model of lysosomal pH regulation. J Gen Physiol 141: 705-720, 2013.
20. DiCiccio JE and Steinberg BE: Lysosomal pH and analysis of the counter ion pathways that support acidification. J Gen Physiol 137: 385-390, 2011.
21. Graves AR, Curran PK, Smith CL and Mindell JA: The Cl-/H+ antiporter ClC-7 is the primary chloride permeation pathway in lysosomes. Nature 453: 788-792, 2008.
22. Leisle L, Ludwig CF, Wagner FA, Jentsch TJ and Stauber T: ClC-7 is a slowly voltage-gated 2Cl(-)/1H(+)-exchanger and requires Ostm1 for transport activity. EMBO J 30: 2140-2152, 2011.
23. Kornak U, Kasper D, Bösl MR, Kaiser E, Schweizer M, Schulz A, Friedrich W, Delling G and Jentsch TJ: Loss of the ClC-7 chloride channel leads to osteopetrosis in mice and man. Cell 104: 205-215, 2001.
24. Kasper D, Planells-Cases R, Fuhrmann JC, Scheel O, Zeitz O, Ruether K, Schmitt A, Poët M, Steinfeld R, Schweizer M, *et al*: Loss of the chloride channel ClC-7 leads to lysosomal storage disease and neurodegeneration. EMBO J 24: 1079-1091, 2005.
25. Steinberg BE, Huynh KK, Brodovitch A, Jabs S, Stauber T, Jentsch TJ and Grinstein S: A cation counterflux supports lysosomal acidification. J Cell Biol 189: 1171-1186, 2010.
26. Majumdar A, Capetillo-Zarate E, Cruz D, Gouras GK and Maxfield FR: Degradation of Alzheimer's amyloid fibrils by microglia requires delivery of ClC-7 to lysosomes. Mol Biol Cell 22: 1664-1676, 2011.
27. Lange PF, Wartosch L, Jentsch TJ and Fuhrmann JC: ClC-7 requires Ostm1 as a beta-subunit to support bone resorption and lysosomal function. Nature 440: 220-223, 2006.
28. Gao G, Chen W, Yan M, Liu J, Luo H, Wang C and Yang P: Rapamycin regulates the balance between cardiomyocyte apoptosis and autophagy in chronic heart failure by inhibiting mTOR signaling. Int J Mol Med 45: 195-209, 2020.
29. Teng M, Jiang XP, Zhang Q, Zhang JP, Zhang DX, Liang GP and Huang YS: Microtubular stability affects pVHL-mediated regulation of HIF-1alpha via the p38/MAPK pathway in hypoxic cardiomyocytes. PLoS One 7: e35017, 2012.
30. Lokuta A, Kirby MS, Gaa ST, Lederer WJ and Rogers TB: On establishing primary cultures of neonatal rat ventricular myocytes for analysis over long periods. J Cardiovasc Electrophysiol 5: 50-62, 1994.
31. Jiang XY, Zhang L, Yu C, Jiang H and Li J: Research for a better method of neonatal rat cardiac myocytes, primary culture and purification. Sichuan Da Xue Xue Bao Yi Xue Ban 46: 301-304, 2015 (In Chinese).
32. Ehler E, Moore-Morris T and Lange S: Isolation and culture of neonatal mouse cardiomyocytes. J Vis Exp 79: 50154, 2013.
33. Fuchsova B, Novak P, Kafkova J and Hozak P: Nuclear DNA helicase II is recruited to IFN-alpha-activated transcription sites at PML nuclear bodies. J Cell Biol 158: 463-473, 2002.
34. Shi B, Huang QQ, Birkett R, Doyle R, Dorfleutner A, Stehlik C, He C and Pope RM: SNAPIN is critical for lysosomal acidification and autophagosome maturation in macrophages. Autophagy 13: 285-301, 2017.
35. Kabeya Y, Mizushima N, Ueno T, Yamamoto A, Kirisako T, Noda T, Kominami E, Ohsumi Y and Yoshimori T: LC3, a mammalian homologue of yeast Apg8p, is localized in autophagosome membranes after processing. EMBO J 19: 5720-5728, 2000.
36. Livak KJ and Schmittgen TD: Analysis of relative gene expression data using real-time quantitative PCR and the 2(-Delta Delta C(T)) method. Methods 25: 402-408, 2001.
37. Kawai A, Uchiyama H, Takano S, Nakamura N and Ohkuma S: Autophagosome-lysosome fusion depends on the pH in acidic compartments in CHO cells. Autophagy 3: 154-157, 2007.
38. Iwai-Kanai E, Yuan H, Huang C, Sayen MR, Perry-Garza CN, Kim L and Gottlieb RA: A method to measure cardiac autophagic flux in vivo. Autophagy 4: 322-329, 2008.
39. Namba DR, Ma G, Samad I, Ding D, Pandian V, Powell JD, Horton MR and Hillel AT: Rapamycin inhibits human laryngotracheal stenosis-derived fibroblast proliferation, metabolism, and function in vitro. Otolaryngol Head Neck Surg 152: 881-888, 2015.
40. Zhang J, Zhou W, Zhu S, Lin J, Wei P, Li F, Jin P, Yao H, Zhang Y, Hu Y, *et al*: Persistency of enlarged autolysosomes underscores nanoparticle-induced autophagy in hepatocytes. Small 13: 1602876, 2017.
41. Yang KC, Sathiyaseelan P, Ho C and Gorski SM: Evolution of tools and methods for monitoring autophagic flux in mammalian cells. Biochem Soc Trans 46: 97-110, 2018.
42. Kurita T, Yamamura H, Suzuki Y, Giles WR and Imaizumi Y: The ClC-7 chloride channel is downregulated by hypoosmotic stress in human chondrocytes. Mol Pharmacol 88: 113-120, 2015.
43. Rabanal-Ruiz Y, Otten EG and Korolchuk VI: mTORC1 as the main gateway to autophagy. Essays Biochem 61: 565-584, 2017.
44. Shen HM and Mizushima N: At the end of the autophagic road: An emerging understanding of lysosomal functions in autophagy. Trends Biochem Sci 39: 61-71, 2014.
45. Mizushima N, Yoshimori T and Levine B: Methods in mammalian autophagy research. Cell 140: 313-326, 2010.
46. Mauvezin C and Neufeld TP: Bafilomycin A1 disrupts autophagic flux by inhibiting both V-ATPase-dependent acidification and Ca-P60A/SERCA-dependent autophagosome-lysosome fusion. Autophagy 11: 1437-1438, 2015.